Supporting Information

One-for-All Nanoplatform for Synergistic Mild Cascade Potentiated Ultrasound Therapy Induced with Targeting-Imaging-Guided Photothermal Therapy

Kai Cheng [1#], Ruo-Yun Zhang [1#], Xiao-Quan Yang [1, 2], Xiao-Shuai Zhang [1], Fang Zhang [1], Jie An [1], Zhuo-Ya Wang [1], Ying Dong [3, 4], Bo Liu [1], Yuan-Di Zhao [1, 2] and Tian-Cai Liu [3, 4*]*

[1] *Britton Chance Center for Biomedical Photonics at Wuhan National Laboratory for Optoelectronics-Hubei Bioinformatics & Molecular Imaging Key Laboratory, Department of Biomedical Engineering, College of Life Science and Technology, Huazhong University of Science and Technology, Wuhan 430074, Hubei, P. R. China*

[2] *Key Laboratory of Biomedical Photonics (HUST), Ministry of Education, Huazhong University of Science and Technology, Wuhan 430074, Hubei, P. R. China*

[3] *Key Laboratory of Antibody Engineering of Guangdong Higher Education Institutes, School of Laboratory Medicine and Biotechnology, Southern Medical University, Guangzhou 510515, Guangdong, P. R. China.*

[4] *Guangdong Provincial Key Laboratory of Construction and Detection in Tissue Engineering, Southern Medical University, Guangzhou 510515, Guangdong, P. R. China.*

[#] *These authors contributed equally to this article.*

** Corresponding author. Tel/Fax: +86-27-8779-2202. Email address: zydi@mail.hust.edu.cn (Y.D. Zhao); liutc@smu.edu.cn (T. C. Liu)*

1. Experimental Section

1.1. Materials. Toluene, acetone and chloroform were purchased from Sinopharm Group Chemical Reagent Co., Ltd; bismuth (III) acetate ($Bi(OAc)_3$), silver acetate (Ag(OAc)), oleic acid (OA, 99%), octadecene and hexamethyldisilathiane were purchased from Aldrich; 1,2-distearoyl-sn-glycero-3-phosphoethanolamine-N-[amino(methoxy polyethylene glycol)$_{2000}$] (DSPE-mPEG$_{2000}$-NH_2) were purchased from Avanti; 1,3-diphenylisobenzofuran (DPBF), thlazolyi blue tetrazolium bromide (MTT) and 2,2,6,6-tetramethylpiperidine (TEMP) were purchased from Aladdin; 2,7-dichlorodi-hydrofluorescein diacetate (DCFH-DA) was purchased from Yi Sheng Biotechnology Co. Ltd; all reagents were of analytical grade, and used without further purification. 4 weeks old BALB/c male mice (SPF grade) and 5 weeks old KM male mice were purchased from Hua Fu Kang Biotechnology Co., Ltd.

1.2. Instruments. CT scan imaging system was constructed by our laboratory. E-scan ^{TM} electron spin resonance spectrometer (Bruker, Switzerland) was used to measure singlet oxygen signal; WFX-200 atomic absorption spectrophotometer (Beijing Beifen-Ruili Analytical Intrument Co., Ltd., China) was to detect concentration of Ag and Bi; elemental analysis of nanoprobe was obtained through AXIS-ULTRA DLD-600W X-ray photoelectron spectrometer (Shimadzu, Japan); WED-100 Ultrasound Therapy (Welld, China) was used as an ultrasound trigger source; quantitative analysis of probe-induced apoptosis and cellular ROS production were proceeded by Cyto FLEX flow cytometer (Beckman Coulter, America); images of cellular fluorescence staining were acquired from FV1000 confocal microscopy (Olympus, Japan); Vertex 70 infrared spectrometer (Bruker, Germany) was to verify the change of functional groups during synthesis of ABS-FA; absorbance detection of MTT was conducted by Elx-808 microplate reader (Biotek, USA); purification of probe was carried out by Concentrator plus (Ependorf, Germany);

MDL-III-808-2.5W laser (Changchun New Industries Optoelectronics Tech. Co., Ltd, China) was used for NIR irradiation; UV-2550 spectrophotometer (Shimadzu, Japan) was to characterize the absorption spectrum of nanoprobe; electron microscopy characterization was performed on Hitachi 120kV HT7700 transmission electron microscope (Hitachi, Japan); particle size and zeta potential were tested by Nano-ZS90 nanometer (Malvern, UK).

1.3. Preparation and concentration detection of $AgBiS_2$ ternary complex. The synthesis of $AgBiS_2$ was in line with the previous literature.[1] At first, 0.39 g $Bi(OAc)_3$ and 0.17 g Ag(OAc) were dissolved in 48 g oleic acid with Ar ptotection, and meanwhile, the mixture was stirred gently and heated to 100˚C remaining 10 h. Then, 5 mL octadecene containing 0.18 g hexamethyldisilathiane was rapidly injected to terminate the reaction and the mixture was slowly cooled down. After that, $AgBiS_2$ was purified using the disperse system (toluene/v: acetone/v=1:1) by three times of centrifugation (12000 rpm for 10 min per time), and lastly dispersed in chloroform. Two aliquots of 10 μL above nanoparticle were dried by Ar, and were next dissolved by adding 100 μL HNO_3 (65%, GR), with further dilution of the nanoparticle to 1% acidity, the concentrations of Bi and Ag were measured by atomic spectrophotometer.

1.4. Preparation of DSPE-mPEG$_{2000}$-FA. The synthesis of DSPE-mPEG$_{2000}$-FA was slightly modified according to literature reported.[2] 40 mg FA was mixed thoroughly with 8 mL DMSO, followed by adding 16 mg DSPE mPEG$_{2000}$-NH_2 (DE-NH_2), 52 mg DCC and 4 mL pyridine in turn. The mixture was gently stirred for 10 h at room temperature, with the solvent pyridine removed in next step by rotary evaporation. The mixture was then dissolved in 20 mL ultrapure water and centrifuged (10000 rpm for 10 min), and repeated for several times to totally discard the precipitation. The obtained supernatant solution was dialyzed (M_w=1000 Da) in 4.2 g/mL $NaHCO_3$ solution (3 L) for 8 times lasting for 4 d, and dialyzed for another 8 times in ultrapure water. The

final solution was lyophilized to obtain yellow powder product, which was kept at -20 ℃ for further use.

1.5. Synthesis of $AgBiS_2$ coated phospholipid with folate-modified (ABS-FA). 20 mg DSPE-$mPEG_{2000}$ and 10 mg DSPE-$mPEG_{2000}$-FA were added to 10 mL chloroform which contained 15 mg $AgBiS_2$, the mixture was stirred at room temperature after sonication for 20 min. After chloroform was completely evaporated, the precipitation was dissolved in 3 mL ultrapure water, and transferred to an ultrafiltration tube (M_w=100 kDa) to remove the excess phospholipid molecule. Finally, the product was dispersed in PBS to obtain $AgBiS_2$@DSPE-$mPEG_{2000}$-FA (ABS-FA). $AgBiS_2$@DSPE-$mPEG_{2000}$-NH_2 (ABS-NH_2) was obtained in the same way as above without the targeted phospholipid DSPE-mPEG2000-FA added.

1.6. Stability and blood compatibility test of ABS-FA. Freeze-dried ABS-FA was divided into 2 equal parts, which were added to PBS and DMEM+10% serum at room temperature, respectively. Then, diameter, polydispersity index (PDI) and zeta potential were measured every 3 d to investigate the stability of ABS-FA. 2 mL fresh blood was obtained from 4 KM mice and transferred into EDTA k2 anticoagulant tube. The supernatant was removed by centrifugation at 700 g for 5 min. After washing several times with physiological saline, 10 μL red blood cell suspension was added into 300 μL ABS-FA solution at systematically varied concentrations (50, 100, 200, 400 and 800 μg/mL), the dissolvant of both were saline. Then, the mixture was incubated in 5% CO_2 atmosphere at 37 ℃ for 1 and 9 h, severally. Next, all suspensions were photographed after centrifugation at 700 g for 5 min. Then, the supernatant of each tube was shifted to 96-well plate, followed by measuring the absorbance at 577 nm. Finally, the cell precipitation was made into cell smear and observed under a microscope. In the above, physiological saline and ultrapure water were served as negative and positive control, individually. The calculation formula of hemolysis rate of

RBCs is as follows equation (eq. 1):

$$\text{Hemolysis Rate (\%)} = (OD_{sample} - OD_{saline})/(OD_{water} - OD_{saline}) \times 100\% \quad (1)$$

1.7. Photothermal, photothermal stability and photothermal conversion efficiency of ABS-FA. 300 μL ABS-FA in different concentrations (0, 0.125, 0.25, 0.5 and 0.75 mg/mL) were irradiated with 808 nm laser (0.75 W/cm^2, 5 min), respectively, and the temperature was recorded by an infrared thermal imager. Similarly, the temperatures regarding 0.75 mg/mL ABS-FA treated with or without NIR irradiation under different powers (0.5, 0.75, 1.0 and 1.25 W/cm^2) were also recorded. Each experiment was repeated four times.

300 μL ABS-FA (0.70mg/mL) in detachable 96-well plate was irradiated with NIR (808 nm, 1.25 W/cm^2) for 5 min and stopped for 10 min to wait the sample cool down. Subsequently, additional 3 NIR on/off cycles were further repeated, and temperature change in each repeat was recorded.

To evaluate the photothermal conversion efficiency, the absorbance of ABS-FA at 808 nm was measured, and 0.3 mL ABS-FA in a quartz cuvette was irradiated with NIR (1.25 W/cm^2, 5 min). Keeping record of temperature change in the whole process was necessary until the solution reached a steady-state temperature. The photothermal conversion efficiency,[3] η, was determined by the following equation (eq. 2):

$$\eta = \frac{hS(T_{Max} - T_{Surr}) - Q_{Dis}}{I(1-10^{-A_{808}})} \quad (2)$$

where h was the heat transfer coefficient, S was the surface area of the container, T_{max} was the highest temperature after irradiation, T_{surr} was the starting temperature, Q_{Dis} was the energy emitted by the solvent, I was the NIR intensity, and A_{808} was the absorbance of the probe at 808 nm).

1.8. CT imaging of ABS-FA *In vitro*. Different concentrations of ABS-FA (0.075, 0.15, 0.3 0.6 and 1.2 mg/mL) and BS-FA (0.075, 0.15, 0.3, 0.6 and 1.2 mg/mL) were used to conduct imaging experiments in self-built CT scan imaging systems.

1.9. Cytotoxicity of probes. HeLa, C26 and 4T1 cells in logarithmic growth phase were inoculated into 96-well plates, which were cultured in 5% CO_2 incubator at 37 ℃ overnight. Next, cells were treated with 200 μL fresh serum-free medium containing different concentrations (0, 1.6, 3.1, 6.25, 12.5, 25, 50, 100 and 200 μg/mL) of ABS-FA, respectively. Six parallel wells were set in each group. After 24 h, the culture medium was removed and the wells were washed three times with PBS, 20 μL thiazole blue (5 mg/mL) was then added into each well with 200 μL fresh free serum medium, which was discarded after another 4 h culture, and 150 μL dimethyl sulfoxide was added per hole. Afterward, absorption at 490 nm was measured by microplate reader after slow shaking for 20 min. The cell viability can be calculated by the following equation (eq. 3):

Cell Viability (%)=(experimental group - blank group)/(control group - blank group)×100%. (3)

1.10. Cellular photothermal and ultrasonic dynamic experiments of ABS-FA. Similarly cultured, 200 μL serum-free medium containing ABS-FA (6.25, 12.5, 25, 50, 100 and 200 μg/mL) was added to HeLa cells in 96-well plates, and removed after 4 h. Then they were washed 3 times with PBS, and treated in different ways (NIR: 0.75 W/cm^2 808 nm laser for 5 min; US: 1.0 W/cm^2 ultrasonic for 2 min), and incubated for another 24 h. Subsequently, 20 μL thiazolyl blue (5 mg/mL) was added to each well. After 4 h, dimethyl sulfoxide was added and absorbance at 490 nm was measured, with cell viability gained.

Under the same culture condition, 500 μL serum-free medium containing ABS-FA (50 μg/mL), separately, was added to HeLa, C26 and 4T1 cells in the confocal culture dish. After 4 h, the culture medium was removed, then washed 3 times and added with PBS. Under the same NIR conditions (1.0 W/cm^2) or ultrasonic (1.0 W/cm^2), the staining solution was removed from the dish after the addition of Calcein-AM and PI for 5 min. Afterwards, they were washed with PBS for 3 times and observed under a confocal microscope. Successively, similar steps were undertaken by only

substituting Calcein-AM and PI with Annexin V-FITC/PI apoptosis staining solution, which discarded remained 15 min before being discarded. Flow cytometry analysis was performed after washing out the staining solution with PBS for 3 times.

Cultured in the same way, 500 μL ABS-FA (50 μg/mL) serum-free medium was added to the 6-well plate seed in HeLa cells. The cells were dealt similarily except for the application of 10 μM DCFH-DA. The cells were next irradiated with NIR (1 W/cm^2) or ultrasound (1.0 W/cm^2). After further incubation for 0.5 h and washing with PBS to remove free DCFH-DA, the cells were observed under fluorescence microscope after 2.5% glutaraldehyde fixation for 30 min. Similarly, the corresponding cells were collected and analyzed quantitatively for DCF fluorescence on a flow cytometer.

1.11. Targeting labeling of ABS-FA. HeLa cells in logarithmic growth phase were seeded in a 6-well plate, which was cultured in 5% CO_2 incubator at 37 ℃ overnight, then 1 mL ABS-FA (50 μg/mL) was added after removing the culture medium. 6 h later, the cells were collected and fixed by 2.5% glutaraldehyde, then the cells were dealt as following steps: (1) rinsed 3 times for 15 min with 0.1 M PBS after 48 h (pH=7.0); (2) fixed with 1% citric acid in PBS (pH=7.4) for 4 h at room temperature; (3) rinsed 3 times for 15 min with PBS (pH=7.4); (4) dehydrated at 30, 50, 70, 80, 85, 90, 95 and 100% alcohol for 20 min; (5) permeated with different ratios (2:1 and 1:1) of acetone and epoxy for 10 h; (6) embedded in an epoxy resin at 60 ℃ for 48 h; (7) made into ultrathin sections about 80 to 100 nm thick using an EM UC7 microtome (Leica, Germany) and observed by TEM.

1.12. Safety test of ABS-FA *in vivo*. 20 four-week-old BALB/c male mice (SPF) were randomly divided into 4 groups. By tail vein injection, the first group was respectively injected with 300 μL ABS-FA (15 mg/mL) at the 1th and 3th d. Similarly, the second group was injected at the 25th and

27th d, and the third group was at the 45th and 47th d. Lastly, the fourth group was injected with 300 μL PBS at the 45th and 47th d. To the end, blood sample were collected and mice were sacrificed, which was used for the blood routine and biochemical analysis. Additionally, mouse organs of the 47th d were obtained and utilized in next HE and CD-68 staining experiments.

1.13. Pharmacokinetic study of ABS-FA. 36 BALB/c nude mice inoculated with HeLa cells were tail vein injected with 200 μL ABS-FA (6 mg/mL), and each 3 mice were sacrificed at 0.1, 1, 3, 6, 8, 10, 12, 24 and 48 h, 5, 9 and 25 d, respectively. Blood, heart, liver, spleen, lung, kidney, small intestine and tumor tissues were taken. Tissues were washed in saline and the residual water was removed by hospital gauze, thus was prepared for further weighing. After that, 400 μL PBS was added into the tubes containing respective tissues for grinding. By adding 5 mL HNO_3 (GR, 65%) in the dark for 1d, digesting at 120 ℃ on digestion apparatus, and the transparent solution was obtained. In the end, contents of Bi and Ag in each tissue was measured at atomic spectrophotometry, by adding diluted nitric acid (2%, GR) to make the capacity at 5 mL.

2. Results and Discussion

2.1. PDT effect of ABS-FA. With ABS-FA concentration and NIR irradiation power varied in compliance with single variable principle. With increasing of probe concentration or NIR irradiation power, results were not disappointing that temperature of ABS-FA was elevated while controlling one of them unchanged at every turn (Figure 2D-F). Enhanced temperature could reach up to 20 ℃ within 5 min (Figure 2F), which was sufficient enough to kill tumor cell, as ABS-FA concentration was 0.75 mg/mL and NIR power was 0.75 W/cm^2 at 808 nm, hence, above parameters were properly chosen for further investigation. Notably, probe concentration and NIR power were both relatively lower, as compared with our previously documented research.[4] Reduplicative and steady

temperature variation, in fact, was correlated with photothermal stability of ABS-FA, thus validating preeminent stability of ABS-FA (0.75 mg/mL), while supplying to cycle- NIR (1.25 W/cm^2, 808 nm) irradiation (Figure 2G).

2.2. Biosafety of ABS-FA *in vitro*. In light of favorable ultrasonic dynamic property, excellent photothermal conversion efficiency, and powerful CT imaging capability of ABS-FA, further application *in vivo* was desired, and hence biosecurity of ABS-FA were studied. Stability was firstly investigated as a prerequisite *in vitro*. Particle size, zeta potential and polymer dispersity index (PDI) of ABS-FA incubating in PBS, dulbecco's modified eagle medium (DMEM) with 10% and 50% fetal bovine serum contained, were determined, separately, at room temperature over time. As a result, these three indicators were basically unaffected in various conditions (Figure S17-19), showing protruding stability of ABS-FA, which laid a sound foundation for its application *in vivo*. It is universally acknowledged, since, that blood is the medium transferring probe into the whole body, blood compatibility of ABS-FA was further explored. By hemolysis experiment of red blood cell (RBC), hemolysis rate of RBC consisted of variant concentrations ABS-FA approached to 0% (Figure 3B), and almost all cells tended to inevitably sink at the bottom, with respective supernatants remained transparent. Similar phenomenon was also observed in physiological saline. In reverse, hemolysis rate of RBC in ultrapure water was 100%, which was possibly due to the differed osmotic pressure. Evidenced by cell smear microscopy, when concentration of ABS-FA was reach up to 0.8 mg/mL and incubated for 9 h, hemolysis rate was still considerable low, and cell morphology was relatively normal, as compared with hemolyzed RBC (Figure 3C), indicating that ABS-FA obtained eminent bioinertness, ultimately guaranteeing innocuousness of subsequent *in vivo* studies for blood circulation system.

To study cytotoxicity of ABS-FA, standardized 3-(4, 5-dimethyl-2-thiazolyl)-2,

5-diphenyl-2-H-tetrazolium bromide, thiazolyl blue tetrazolium bromide (MTT) experiments were conducted with three kinds of tumor cells. ABS-FA with varied concentrations were incubated with HeLa, C26 and 4T1 cells for 24 h, respectively. They all featured with high survival rates (81.16, 89.39 and 89.63%, respectively), even when concentration topped up to 100 μg/mL (Figure 3D), hinting that ABS-FA exhibited outstanding biocompatibility and pimping toxicity. At the same concentration, ABS-FA was slightly more noxious to HeLa cells, generating greater suppressive impact on cell viability than C26 and 4T1 cells, which could be explained by larger intake of targeting probe for HeLa cells, and inhibiting activity of cells later. All above data confirmed that the designed ABS-FA was with fairly convincing biosafety *in vitro*, which laid sound foundation for further application of tumor therapy *in vivo*.

2.3. Detection Principle of ROS. In principle, DCFH-DA can be hydrolyzed by intracellular esterase to form dichlorodihydrofluorescein diacetic acid (DCFH), which cannot possess ability of penetrating cell membrane. While ROS appears, DCFH can be oxidized to form fluorescent dichlorofluorescein (DCF), thus making ROS observable under microscopy. Therefore, production of ROS was investigated by different probes.

2.4. Properties of $AgBiS_2$ nanoparticle. For $AgBiS_2$ nanoparticle, electron spin resonance experiment under the same concentration conditions was conducted. It was clear that the triplet signal peak of $AgBiS_2$ group did not change significantly comparing with ABS-FA (Figure 2A), showed that modification of DSPE-PEG_{2000}-FA did not significantly reduce the ultrasonic dynamics effect of $AgBiS_2$. When $AgBiS_2$ (0.25 mg/mL) co-incubated with DPBF and treated with ultrasonic (0.5 W/cm^2) for 2 min, absorption value of $AgBiS_2$ group (Figure S13) decreased at 415 nm was basically the same as ABS-FA group's, which meant that wrapping with DSPE-PEG_{2000}-FA made negligible difference to ultrasonic. When $AgBiS_2$ (0.25 mg/mL) was irradiated with NIR (0.75

W/cm^2) for 5 min, it was found that temperature rise curve of $AgBiS_2$ (Figure S14) was almost the same as that of ABS-FA. Furthermore, the photothermal conversion efficiency of $AgBiS_2$ in chloroform solution was explored, that was, UV-vis absorption spectrometer was to measure the absorption value of $AgBiS_2$ nanoparticle at 808 nm, and meanwhile took 300 μL $AgBiS_2$ solution for NIR irradiation (500 mW, five min), then cooled down (10 min), and recorded the temperature change (Figure S15 and S16) in whole process. After calculating with eq. 2, η=38.6%, which was close to that of ABS-FA (37.4%). In summary, the wrapped DSPE-PEG_{2000}-FA had no greater effect on the properties of $AgBiS_2$ nanoparticle

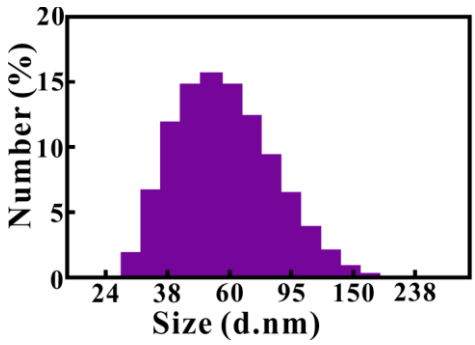

Figure S1. Dynamic light scattering of ABS-FA.

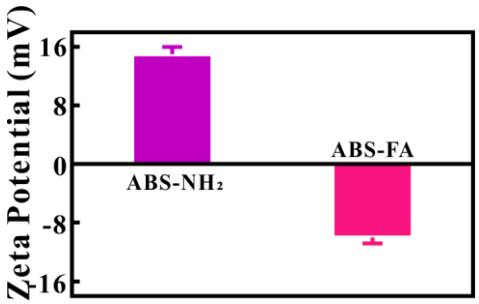

Figure S2. Zeta potentials of $ABS-NH_2$ and ABS-FA.

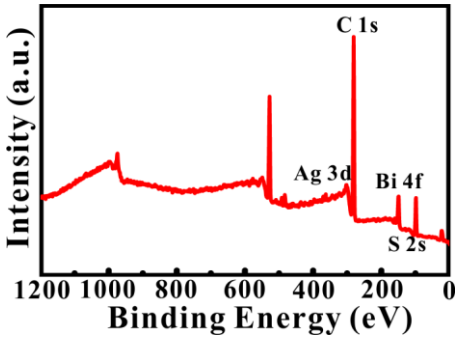

Figure S3. XPS spectra of ABS-FA.

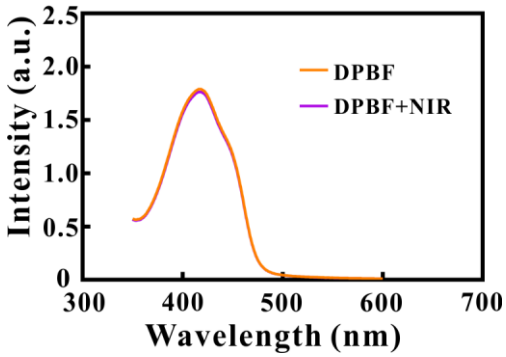

Figure S4. Absorption spectra of DPBF before and after treatment with NIR irradiation (0.5 W/cm^2) for 2 min.

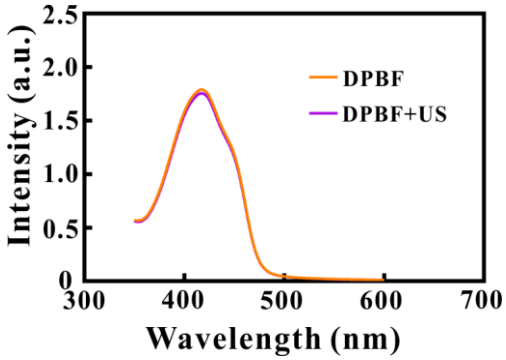

Figure S5. Absorption spectra of DPBF before and after treatment with ultrasonic power (0.5 W/cm^2) for 2 min.

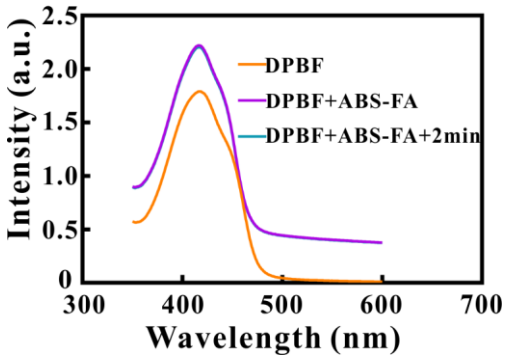

Figure S6. Absorption spectra of ABS-FA co-incubated with DPBF and treated for 2 min.

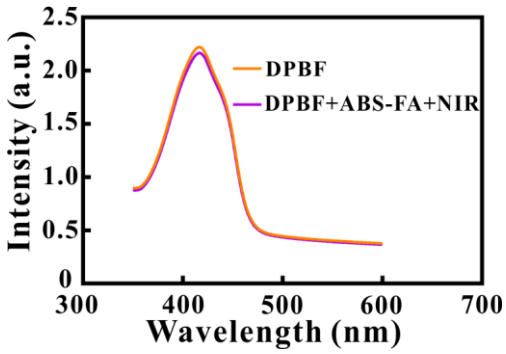

Figure S7. Absorption spectra of ABS-FA co-incubated with DPBF and treated with NIR irradiation (0.5 W/cm^2) for 2 min.

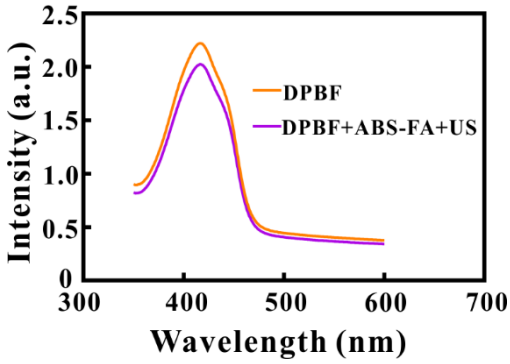

Figure S8. Absorption spectra of ABS-FA co-incubated with DPBF and treated with ultrasonic power (0.5 W/cm^2) for 2 min.

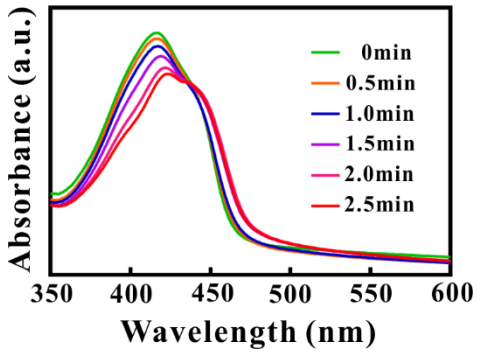

Figure S9. Absorption spectra of DPBF co-incubation with ABS-FA treated with different ultrasonic time (0, 0.5, 1.0, 1.5, 2.0 and 2.5 min).

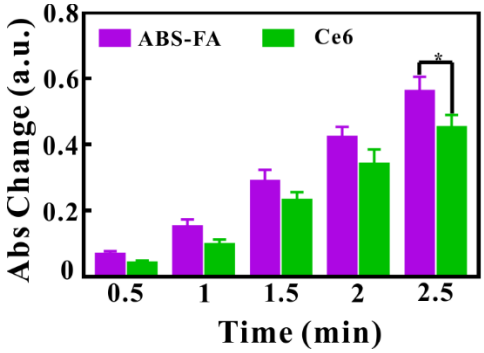

Figure S10. Intensity change of DPBF absorption at 415 nm before and after ABS-FA and Ce6 treated with different ultrasonic time.

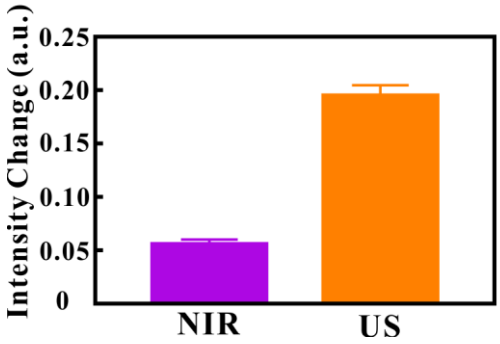

Figure S11. Intensity change of DPBF absorption at 415 nm before and after ABS-FA treated with NIR and US for 2 min.

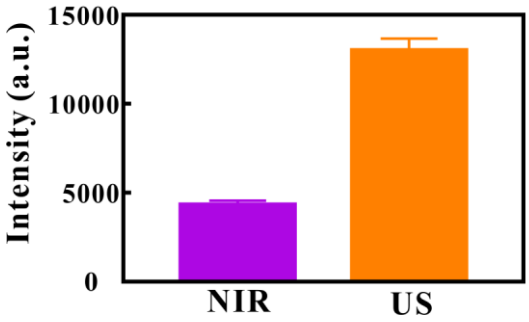

Figure S12. Peak intensity of TEMP after ABS-FA treated with NIR and US at the same condition.

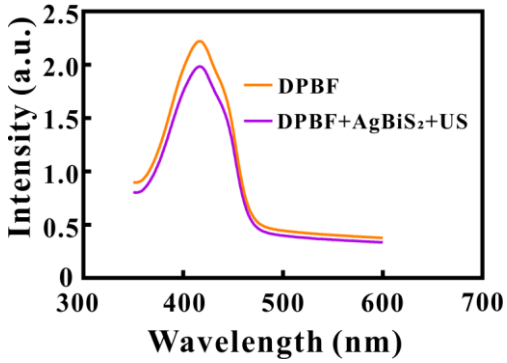

Figure S13. Absorption spectra of $AgBiS_2$ co-incubated with DPBF and treated with ultrasonic power (0.5 W/cm^2) for 2 min.

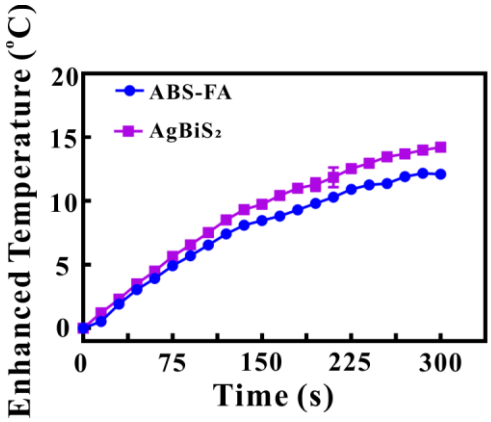

Figure S14. Enhanced temperature of ABS-FA and $AgBiS_2$ (0.25 mg/mL) under NIR (0.75W/cm^2) irradiation.

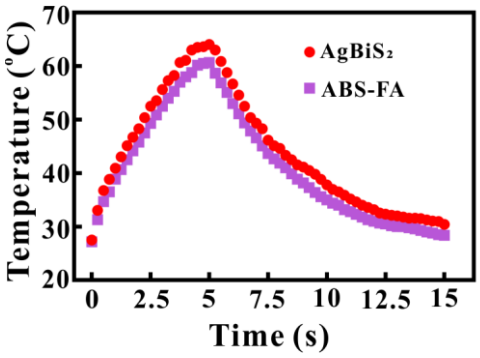

Figure S15. Temperature changes of ABS-FA and $AgBiS_2$ with/without NIR (500 mW) irradiation.

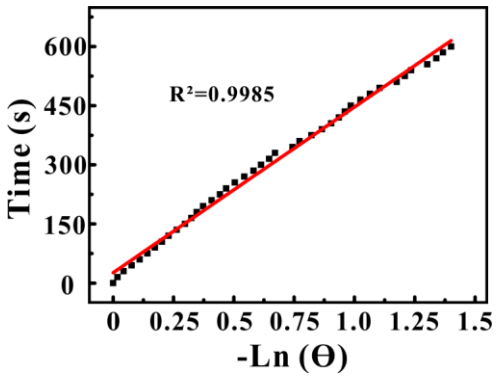

Figure S16. Calculation of τ in photothermal conversion efficiency.

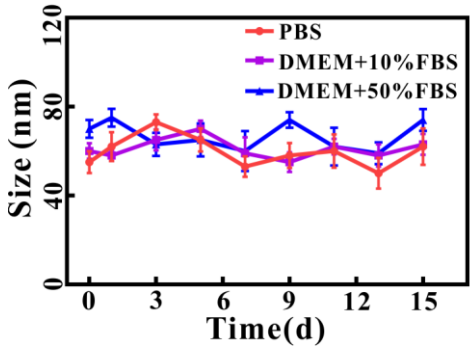

Figure S17. Particle size of ABS-FA incubated with PBS, DMEM+10% and 50% fetal bovine serum varied with time.

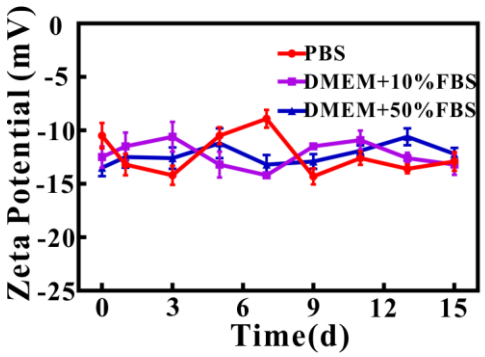

Figure S18. Zeta potential of ABS-FA incubated with PBS, DMEM+10% and 50% fetal bovine serum varied with time.

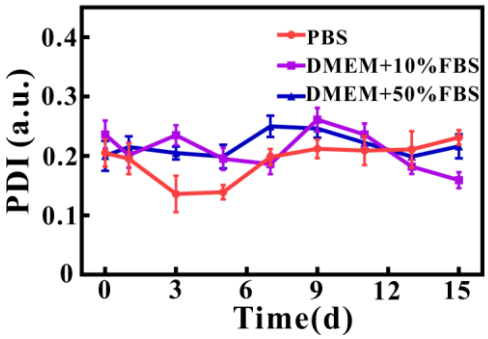

Figure S19. PDI of ABS-FA incubated with PBS, DMEM+10% and 50% fetal bovine serum varied with time.

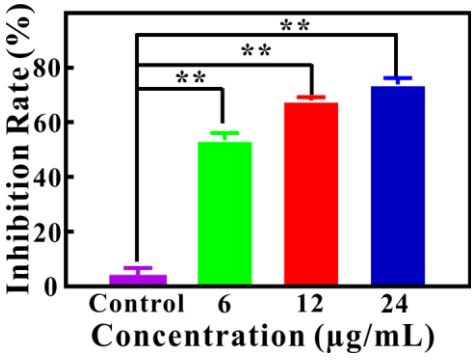

Figure S20. Cell migration Inhibition rate of ABS-FA incubated with HeLa cells for varied times (0, 6, 24 and 48h) with diverse concentrations (0, 6, 12 and 24 μg/mL).

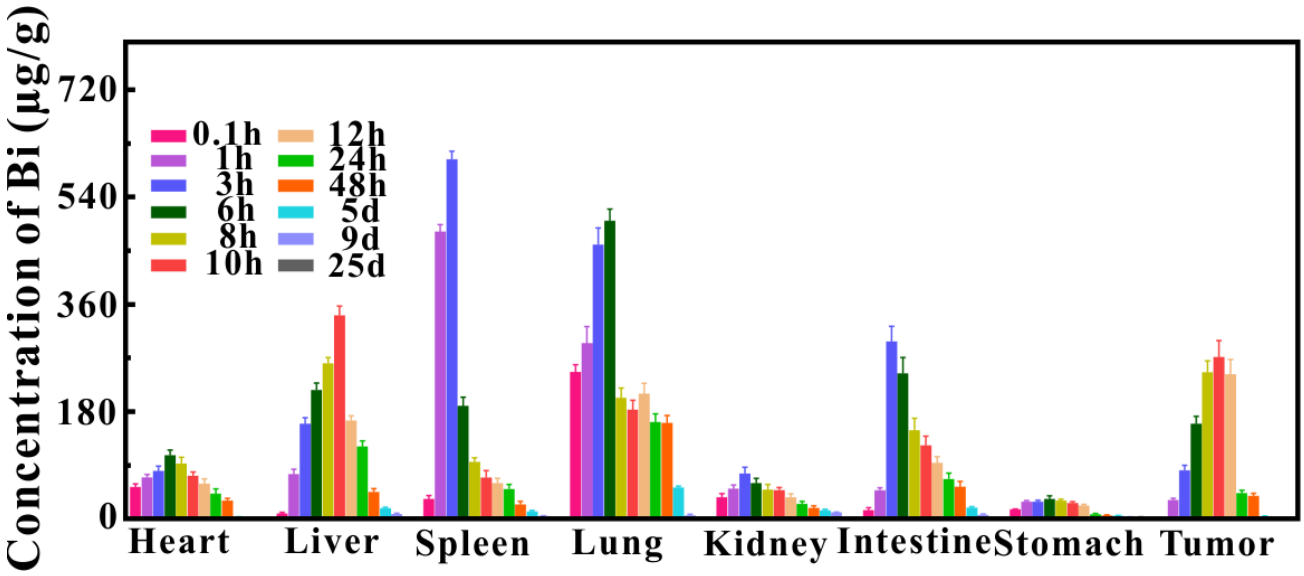

Figure S21. Contents change vs. time of Bi in tumor and organs after injection of ABS-FA into HeLa tumor-bearing mice.

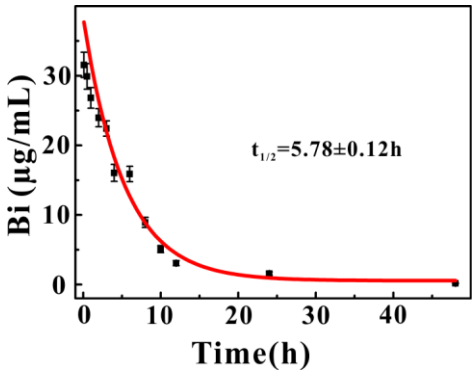

Figure S22. The change of Bi during blood circulation over time.

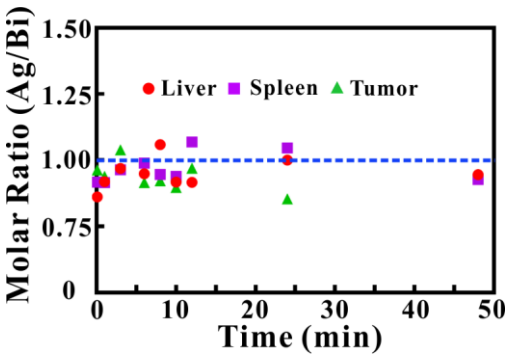

Figure S23. Molar ratio of Ag to Bi in each organ at the same time.

Figure S24. White-light images of HeLa tumor-bearing mice after different treatments and observations at different times.

REFERENCES

(1) Bernechea, M.; Miller, N. C.; Xercavins, G.; So, D.; Stavrinadis, A.; Konstantatos, G. Solution-Processed Solar Cells Based on Environmentally Friendly $AgBiS_2$ Nanocrystals. *Nat. Photonics* **2016**, *10*, 521-525.

(2) Gabizon, A.; Horowitz, AT.; Goren, D.; Tzemach, D.; Mandelbaum-Shavit, F.; Qazen, MM.; Zalipsky, S. Targeting Folate Receptor with Folate Linked to Extremities of Poly(ethylene glycol)-Grafted Liposomes: in Vitro Studies. *Bioconjugate Chem.* **1999**, *10*, 289-298.

(3) Yang, H.; Zhao, J.; Wu, C.; Ye, C.; Zou, D.; Wang, S. Facile Synthesis of Colloidal Stable MoS_2 Nanoparticles for Combined Tumor Therapy. *Chem. Eng. J.* **2018**, *351*, 548-558.

(4) Cheng, K.; Yang, X.-Q.; Zhang, X.-S.; Chen, J.; An, J.; Song, Y.-Y.; Li, C.; Xuan, Y.; Zhang, R.-Y.; Yang, C.-H.; Song, X.-L.; Zhao, Y.-D.; Liu. B. High-Security Nanocluster for Switching Photodynamic Combining Photothermal and Acid-Induced Drug Compliance Therapy Guided by Multimodal Active-Targeting Imaging. *Adv. Funct. Mater.* **2018**, *28*, 1803118.